Disproportionation and Metallization at Low-Spin to High-Spin Transition in Multiorbital Mott Systems

Jan Kuneš and Vlastimil Křápek

Institute of Physics, Academy of Sciences of the Czech Republic, Cukrovarnická 10, Praha 6, 162 53, Czech Republic

(Received 11 March 2011; published 21 June 2011)

We study the thermally driven spin state transition in a two-orbital Hubbard model with crystal-field splitting, which provides a minimal description of the physics of $LaCoO_3$. We employ the dynamical mean-field theory with a quantum Monte Carlo impurity solver. At intermediate temperatures we find a spin disproportionated phase characterized by a checkerboard order of sites with small and large spin moments. The high temperature transition from the disproportionated to a homogeneous phase is accompanied by a vanishing of the charge gap. With the increasing crystal-field splitting the temperature range of the disproportionated phase shrinks and eventually disappears completely.

DOI: 10.1103/PhysRevLett.106.256401 PACS numbers: 71.10.Fd, 71.28.+d, 71.30.+h, 75.30.Wx

The pressure or thermally driven spin state transitions play an important role in the physics of magnetic oxides [1]. A notorious example is $LaCoO_3$. Its peculiar magnetic and transport properties have attracted the attention of physicists for decades, yet the interpretation of its behavior remains controversial. The main characteristics of $LaCoO_3$ are the temperature (T) dependencies of the magnetic susceptibility and the conductivity [2,3], which exhibit three distinct regions: (i) a low-T nonmagnetic insulator, (ii) an intermediate-T paramagnetic insulator, and (iii) a high-T paramagnetic bad metal. It is generally believed that the evolution from the nonmagnetic to the paramagnetic state is due to thermal population of an excited state of the Co ion with spin (or spin and orbital) degeneracy. Commonly considered scenarios involve either low-spin to high-spin excitation [2,4–6], low-spin to intermediate-spin excitation, [7] or both [8,9]. Temperature affects the electronic system also indirectly, by changing the crystal-field splitting through the lattice thermal expansion. Yet another piece to the puzzle is the deformation of CoO_6 octahedra and their coupling to the spin states of the Co ion [2,8]. Therefore it is rather difficult to distinguish the leading effects from the secondary ones.

In this Letter we study a minimal fermionic lattice model that exhibits the spin state transition. As purely electronic it does not include the effect of lattice thermal expansion or the magnetoelastic coupling. The model is a simplified version of the one studied by Werner and Millis [10], who used the dynamical mean-field theory [11] (DMFT) to map out its phase diagram at fixed temperature, and by Suzuki, Watanabe, and Ishihara [12], who studied its ground state as a function of doping by variational Monte Carlo simulations. We employ the DMFT method to study the temperature-dependent properties in the vicinity of the boundary between the low-spin and high-spin phases. Unlike Ref. [10] we assume a specific lattice, which allows us to investigate the ordering tendencies. We compute the one-particle spectra and the local as well as the uniform spin susceptibility and find that, similar to the behavior of $LaCoO_3$, the model exhibits three distinct temperature regions. In addition to the low-T nonmagnetic insulator and high-T local moment metal we find a spin disproportionated insulating phase at intermediate temperatures. In order to interpret the DMFT results we construct an effective low-energy model, which allows analytic calculations.

Our starting point is a two-orbital Hubbard Hamiltonian on a square lattice

$$H = \sum_{i,\sigma}[(\Delta-\mu)n^a_{i,\sigma} - \mu n^b_{i,\sigma}] + \sum_{\langle ij\rangle,\sigma}(t_{aa}a^\dagger_{i,\sigma}a_{j,\sigma} + t_{bb}b^\dagger_{i,\sigma}b_{j,\sigma}) + U\sum_i(n^a_{i,\uparrow}n^a_{i,\downarrow} + n^b_{i,\uparrow}n^b_{i,\downarrow}) + (U-2J)\sum_{i,\sigma}n^a_{i,\sigma}n^b_{i,-\sigma} + (U-3J)\sum_{i,\sigma}n^a_{i,\sigma}n^b_{i,\sigma}, \quad (1)$$

where $a^\dagger_{i,\sigma}$, $b^\dagger_{i,\sigma}$ ($a_{i,\sigma}$, $b_{i,\sigma}$) are the fermionic creation (annihilation) operators for a spin index σ and two types of orbitals for each lattice site i, and $n^a_{i,\sigma}$, $n^b_{i,\sigma}$ are the corresponding occupation number operators. The nearest-neighbor hoppings $t_{aa} = 0.45$ eV, $t_{bb} = 0.05$ eV and the on-site interaction parameters $U = 4$ eV and $J = 1$ eV are chosen to yield a broad a band and a narrow b band, mimicking the electronic structure of $LaCoO_3$. The crystal-field splitting is denoted with Δ. The T-dependent chemical potential μ is fixed to yield the average filling of 2 electrons per lattice site. Unlike Ref. [10] we consider only Ising terms in the on-site interaction.

The context of the present study is set by a conceptual form [13] of the U-Δ phase diagram of Ref. [10] shown in Fig. 1. The boundary of the metallic phase is given by the opening of a linearly increasing charge gap (indicated by the color intensity). The line separating the high-spin (HS) Mott and low-spin (LS) band insulator corresponds to degeneracy of local HS and LS states. The parameter range of interest corresponding to small gap LS insulator is close

 © 2011 American Physical Society

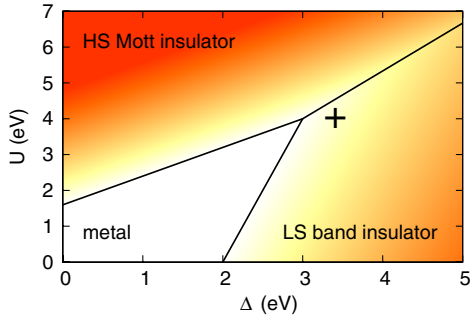

FIG. 1 (color online). Conceptual phase diagram of the two-band model for $U/J = 4$. The size of the charge gap is indicated by color intensity (white = no gap). The parameters of the present study are marked with the cross.

to the triple point. In the following we present the results for Δ of 3.40 and 3.42 eV (marked with the cross in Fig. 1). The DMFT equations are solved as described in Ref. [14] using the strong coupling continuous time quantum Monte Carlo solver [15]. Guided by proposals of spin disproportionation in $LaCoO_3$ [2,16] we have doubled ($\sqrt{2} \times \sqrt{2}$) the unit cell to allow for a spontaneous two-sublattice order (the sublattices are denoted with A and B). All results presented below are in the paramagnetic phase. Although we have checked for a 2×2 antiferromagnetic order in the disproportionated phase at several temperatures, it was never found stable.

In Fig. 2(b) we show the T-dependent occupancies $\bar{n}^a_{A,B}$. Below 500 K a disproportionation takes place. We demonstrate the typical behavior on the two sublattices by showing the contribution of the local eigenstates to the partition function and the imaginary time spin-spin correlation function $\langle s_z(\tau) s_z(0) \rangle$ for the case $\Delta = 3.40$ eV and $T = 290$ K. The A sites, Fig. 2(c), host a statistical mixture of LS ($a^0 b^2$) and HS ($a^1 b^1$) states with short excursions to 1-electron ($a^0 b^1$) configuration, which contributes only to the rapidly decaying part of $\langle s_z(\tau) s_z(0) \rangle$. The HS weight is strongly suppressed on the B sites, Fig. 2(d), which host the LS ($a^0 b^2$) states with short excursions to 3-electron ($a^1 b^2$) configurations. The weight of the HS state translates directly to the magnitude of the constant part of $\langle s_z(\tau) s_z(0) \rangle$ and thus to the local spin susceptibility, given by $\int_0^\beta d\tau \langle s_z(\tau) s_z(0) \rangle$.

In Fig. 2(a) we show the site-averaged local spin susceptibility while the site-resolved contributions are presented in the inset. Comparison to the local spin susceptibility calculated in the (by constraint) homogeneous phase reveals an enhancement of the average HS abundance due to the disproportionation. We have calculated also the uniform spin susceptibility. In the disproportionated phase the uniform spin susceptibility nearly coincides with the average local susceptibility, which is a simple consequence of the local moments on A sites being separated from each other by the B sites hosting the LS singlets. In the high-T homogeneous phase the uniform

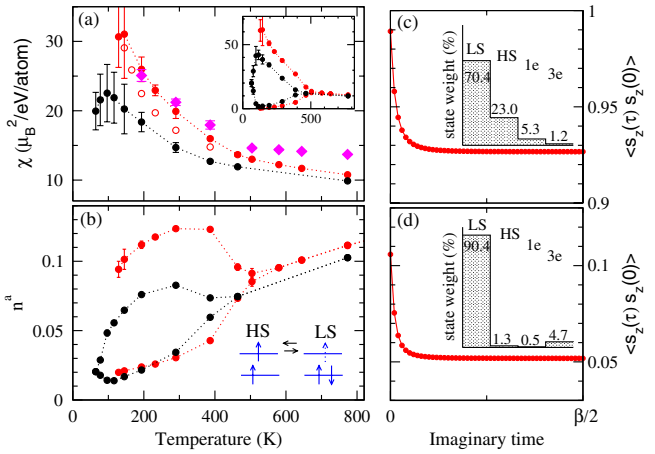

FIG. 2 (color online). (a) The T dependence of the site-averaged local spin susceptibility (filled circles) for Δ of 3.40 [gray (red)] and 3.42 (black) eV. The corresponding site-resolved contributions are shown in the inset. The $\Delta = 3.40$ eV data are compared to the uniform susceptibility (diamonds) and the local susceptibility obtained in the homogeneous phase (empty circles). (b) The site-resolved occupancy $\bar{n}^a$ (the same color coding as above). (c,d) The spin-spin correlation functions on sites A (c) and B (d) for $\Delta = 3.40$ eV and $T = 290$ K. (Note the different intervals on the vertical axis covered in the two graphs.) The column charts show the contributions of the different local eigenstates described in the text.

susceptibility is found to be enhanced over its local counterpart. This is somewhat counterintuitive since a naive expectation of an antiferromagnetic superexchange between the neighboring HS excitations should lead to an opposite effect. The Pauli susceptibility associated with the bad metallic state, discussed next, is an order of magnitude too small to provide an explanation.

The evolution of the one-particle spectra is shown in Fig. 3. The disproportionated phase exhibits a well-defined

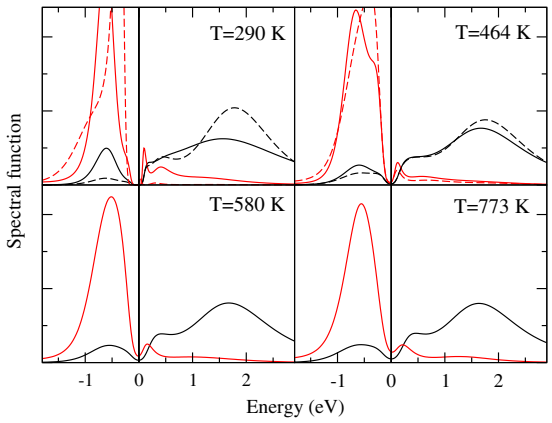

FIG. 3 (color online). The T evolution of the one-particle spectra for $\Delta = 3.40$. The spectral densities of different orbitals are resolved by color: a (black) and b [gray (red)], while the dashed lines correspond to the B sites and full lines to the A sites.

charge gap which starts to fill with incoherent excitations as the system approaches the transition to the homogeneous phase. To interpret this behavior we consider the definition of the charge gap in terms of the eigenenergies of the system $E_{N+1} + E_{N-1} - 2E_N$, where E_N corresponds to an eigenstate with a nonvanishing occupancy and E_{N+1}, E_{N-1} are energies of lowest states that can be reached by adding or removing an electron. At zero temperature the ground state is a product of LS (a^0b^2) configurations on each site. The lowest $N+1$ state corresponds to a single a electron propagating over the filled b band, while the lowest $N-1$ state corresponds to a single b hole. The gap is obtained as the on-site contribution reduced by half-bandwidths $U - 5J + \Delta - W_a/2 - W_b/2$.

The situation at elevated temperatures is more complicated as the initial states involve also sites in HS configuration as well as sites with one or three electrons. The disproportionated and the homogeneous phases differ in the constraints posed on the relaxation of $N+1$ and $N-1$ excitations by the states of the neighboring sites. While in the homogeneous phase each site has neighbors which fluctuate into 1- and 3-electron states, in the disproportionated phase fluctuations are either to 1-electron states on A sites or 3-electron states on B sites. As an example we discuss the b-electron excitations on an A site from the HS initial configuration. (The LS initial configurations contribute with a completely filled valence band.) In the disproportionated phase the energy of the lowest $N+1$ state reached by adding a b electron consists of the on-site contribution reduced by $W_a/2$ due to a electron hopping. The lowest $N-1$ state reached by b electron removal corresponds to (a^1b^1) configuration on the A site and (a^0b^1) configuration on the neighboring B site. The corresponding gap estimate is still finite $(U - 2J - W_a/2)$. In the homogeneous phase the lowest $N-1$ excitation connected with b electron removal is the same as just mentioned. For $N+1$ excitations there is an additional possibility in the homogeneous phase to add the b electron on a site in the HS state while its neighbor is in the (a^0b^1) configuration leading to the (a^0b^2) final state with (a^1b^1) on the neighboring site after a electron transfer. Considering these excitations we obtain a vanishing estimate for the charge gap.

To gain insight into the DMFT results we integrate out the charge fluctuations in (1) to get an effective classical model with three low-energy states (LS, HS ↑, HS ↓):

$$\tilde{H} = \xi_0 \sum_{i,\sigma} n^{\mathrm{HS}}_{i,\sigma} + \sum_{\langle ij\rangle,\sigma} (\xi_1 n^{\mathrm{LS}}_i n^{\mathrm{HS}}_{j,\sigma} + \xi_2 n^{\mathrm{HS}}_{i,\sigma} n^{\mathrm{HS}}_{j,-\sigma}). \quad (2)$$

Here $n^{\mathrm{HS}}_{i,\sigma}$ and n^{LS}_i are the projectors on the three states, and $\langle ij\rangle$ denote summation over all oriented nearest-neighbor bonds. The coupling constants arising from virtual hopping read $\xi_0 = \Delta - 3J$, $\xi_1 = -\frac{t^2_{aa}+t^2_{bb}}{U-2J}$, and $\xi_2 = -\frac{t^2_{aa}+t^2_{bb}}{U+J}$. It should be pointed out that this model is only good for qualitative comparison to the DMFT data as the charge fluctuations are not negligible (in particular in the metallic phase). A mean-field decoupling of (2) allowing for a two-sublattice order leads to the free energy per site

$$F(T) = \frac{\xi_0}{2}(x_A + x_B) + 2\xi_1(x_A + x_B - 2x_A x_B) - \xi_2 x_A x_B + \frac{T}{2}(1 - x_A)\ln(1 - x_A) + \frac{T}{2}(1 - x_B)\ln(1 - x_B) + \frac{T}{2}x_A \ln\left(\frac{x_A}{2}\right) + \frac{T}{2}x_B \ln\left(\frac{x_B}{2}\right), \quad (3)$$

where $x_{A,B}$ are the mean values of $n^{\mathrm{HS}}_\uparrow + n^{\mathrm{HS}}_\downarrow$ on the two sublattices. The equilibrium values of $x_A - x_B$ obtained by minimization of (3) are shown in Fig. 4 together with the corresponding uniform spin susceptibility. For $\xi_0 > 4\xi_1$ we find a uniform LS ground state at $T = 0$, which is followed by a transition into the disproportionated phase characterized by $x_A \neq x_B$ between temperatures T_{c1} and T_{c2}. With increasing ξ_0 the T_{c1} and T_{c2} converge and the disproportionated phase eventually disappears for large enough ξ_0. This result shows that the driving for the observed disproportionation is an attractive superexchange interaction between the HS and LS states depicted in Fig. 2(b).

The disproportionated phase exhibits an enhanced susceptibility, which has two sources. First, like in the DMFT results the HS abundance is enhanced with respect to the homogeneous phase. Second, in the homogeneous phase the antiferromagnetic coupling ξ_2 reduces the uniform susceptibility. Note that this is in contrast to the DMFT results.

The HS-LS model is not new. It was suggested for $LaCoO_3$ by Raccah and Goodenough [2] and the disproportionation was studied by Bari and Sivardière [17]. However, traditionally the interaction between the LS and HS state was associated with the magnetoelastic coupling, namely, a breathing distortion of the CoO_6

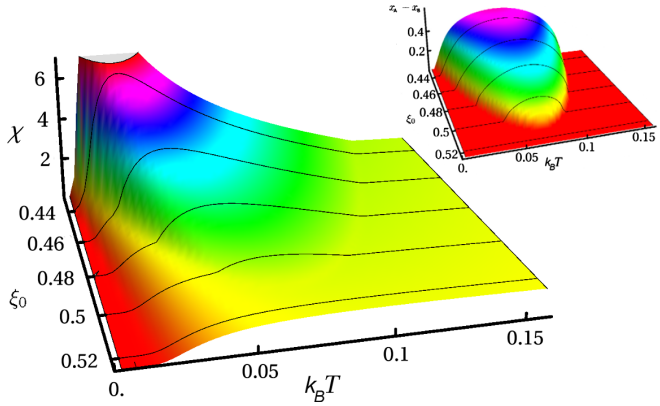

FIG. 4 (color online). The uniform susceptibility of the classical model as a function of temperature and the parameter ξ_0. The inset shows the difference of the HS populations $x_A - x_B$ as a function of temperature and ξ_0.

octahedra. This is quite different from the present work where the disproportionation is of purely electronic origin.

Finally, we discuss the implications of our results in the context of $LaCoO_3$. We have shown that physics of $LaCoO_3$ over the whole temperature range can be qualitatively described by purely electronic effects and with only one local moment state. The simplicity of the present model lends it generality, but inevitably involves approximations. First, our model has two nondegenerate orbitals while $LaCoO_3$ is characterized by threefold quasidegenerate t_{2g} and twofold degenerate e_g orbitals leading to different entropic contributions. Nevertheless, the main control parameters are the coupling constants, and different band degeneracies have only quantitative effect. Second, the Co-O bond lengths change due to the normal and anomalous lattice thermal expansion [8]. The latter is caused by populating the HS state, well-known to weaken the metal ion-ligand bonds [18,19]. Considering a path of decreasing $\xi_0(T)$ in Fig. 4 it is clear that the lattice response enhances the observed effects as a smaller crystal field favors the disproportionation as well as the metallization. Third, no disproportionation and corresponding breathing lattice distortion was observed in recent experiments [8,20]. It is well-known that mean-field approximations overestimate ordering tendencies and that a long-range order in the mean-field solution is often indicative of short-range correlations in the system. Therefore we speculate that in $LaCoO_3$ dynamical HS-LS correlations take place. It is plausible that such a dynamical effect can arise from the instantaneous HS-LS interaction of electronic origin. On the other hand, for the magnetoelastic HS-LS interaction the retardation effects due to the lattice dynamics are likely to weaken dynamical HS-LS correlation considerably. Fourth, two regions of Curie-Weiss behavior observed in experiments have been interpreted as evidence for two different local moment states (high-spin and intermediate-spin) [9]. In our model we observe different behaviors of the uniform susceptibility in the disproportionated and in the homogeneous high-T phase. The difference has three sources: (i) an enhanced abundance of the HS configurations in the disproportionated phase (over a hypothetical homogeneous phase at the same T), (ii) absence of the nearest-neighbor antiferromagnetic correlations in the disproportionated phase, (iii) the metallicity of the homogeneous phase.

In conclusion, we have used numerical DMFT method to study a two-band Hubbard model with quasidegenerate high-spin and low-spin local states. Varying temperature we have observed three different regimes: a low-spin insulator, an insulating phase with HS-LS disproportionation and enhanced Curie-Weiss susceptibility, and a homogeneous metallic phase with Curie-Weiss susceptibility. We have argued that our model study captures the essential physics of $LaCoO_3$ and thus that the properties of $LaCoO_3$ can be explained with a single magnetic moment carrying state and without the effect of the lattice thermal expansion.

We thank Z. Jirák and P. Novák for numerous discussions and P. Werner for providing the QMC impurity solver. This work was supported by the Grant No. P204/10/0284 of the Grant Agency of the Czech Republic and by the Deutsche Forschungsgemeinschaft through FOR1346.

Note added in proof.—After acceptance of our Letter we realized that the classical model (2) is equivalent to the Blume-Emery-Griffiths model [21] with a repulsive biquadratic term.

[1] P. Gütlich and H. A. Goodwin, *Spin Crossover in Transition Metal Compounds I* (Springer-Verlag, Berlin, 2004).
[2] P. M. Raccah and J. B. Goodenough, Phys. Rev. **155**, 932 (1967).
[3] K. Asai *et al.*, Phys. Rev. B **50**, 3025 (1994).
[4] R. R. Heikes, R. C. Miller, and R. Mazelsky, Physica (Amsterdam) **30**, 1600 (1964).
[5] C. S. Naiman *et al.*, J. Appl. Phys. **36**, 1044 (1965).
[6] A. Podlesnyak *et al.*, Phys. Rev. Lett. **97**, 247208 (2006).
[7] M. A. Korotin *et al.*, Phys. Rev. B **54**, 5309 (1996).
[8] P. G. Radaelli and S.-W. Cheong, Phys. Rev. B **66**, 094408 (2002).
[9] K. Asai *et al.*, J. Phys. Soc. Jpn. **67**, 290 (1998).
[10] P. Werner and A. J. Millis, Phys. Rev. Lett. **99**, 126405 (2007).
[11] A. Georges *et al.*, Rev. Mod. Phys. **68**, 13 (1996).
[12] R. Suzuki, T. Watanabe, and S. Ishihara, Phys. Rev. B **80**, 054410 (2009).
[13] J. Kuneš *et al.*, Eur. Phys. J. Special Topics **180**, 5 (2010).
[14] J. Kuneš *et al.*, Phys. Rev. B **75**, 165115 (2007).
[15] P. Werner *et al.*, Phys. Rev. Lett. **97**, 076405 (2006); A. Albuquerque *et al.*, J. Magn. Magn. Mater. **310**, 1187 (2007).
[16] K. Knížek *et al.*, Phys. Rev. B **79**, 014430 (2009).
[17] R. A. Bari and J. Sivardière, Phys. Rev. B **5**, 4466 (1972).
[18] J. Badro *et al.*, Phys. Rev. Lett. **89**, 205504 (2002).
[19] J. Kuneš *et al.*, Phys. Rev. Lett. **102**, 146402 (2009).
[20] G. Maris *et al.*, Phys. Rev. B **67**, 224423 (2003).
[21] M. Blume, V. J. Emery, and R. B. Griffiths, Phys. Rev. A **4**, 1071 (1971).